14

Neural Network Control of Non-linear Full Vehicle Model Vibrations

Rahmi Guclu and Kayhan Gulez
Yildiz Technical University
Turkey

1. Introduction

Vehicle suspension serves the basic function of isolating passengers and the chassis from the roughness of the road to provide a more comfortable ride. In other words, very important role of the suspension system is the ride control. Due to developments in the control technology, electronically controlled suspensions have gained more interest. These suspensions have active components controlled by a microprocessor. By using this arrangement, significant achievements in vehicle response can be carried out. Selection of the control method is also important during the design process. In this study, Neural Network (NN) controllers parallel to McPherson strut-type independent suspensions are used. The major advantages of this control method are its success, robust structure and the ability and adaptation of using these types of controllers on vehicles. To simplify models, a number of researchers assumed vehicle models to be linear. However, such models ignore non-linearities present in the system. By including non-linearities such as dry friction on dampers, the results become more realistic.

During the last decade, many researchers applied some linear and non-linear control methods to vehicle models. Due to simplicity, quarter car models were mostly preferred. (Redfield & Karnopp, 1998) examined the optimal performance comparisons of variable component suspensions on a quarter car model. (Yue et al., 1989) also applied LQR and LQG controller to a quarter car model.

(Stein & Ballo, 1991) designed a driver's seat for off-road vehicles with active suspensions. Hac (Hac, 1992) applied optimal linear preview control on the active suspensions of a quarter car model. (Rakheja et al., 1994) added a passenger seat in their analysis. A passenger seat suspension system was described by a generalized two degrees of freedom model and with non-linearities such as shock absorber damping, linkage friction and bump stops. Since the quarter car model is insufficient to give information about the angular motions of a vehicle, some researchers used more complex models like half and full car models. These models give information about the pitch, roll and bounce motions of a vehicle body. (Crolla & Abdel Hady, 1991) compared some active suspension control laws on a full car model. Integrated or filtered white noise was taken as the road input. The same researchers applied linear optimal control law to a similar model in 1992. (Hrovat, 1993) compared the performances of active and passive suspension systems on quarter, half and full car models using linear quadratic optimal control.

Source: Vibration Control, Book edited by: Dr. Mickaël Lallart,
ISBN 978-953-307-117-6, pp. 380, September 2010, Sciyo, Croatia, downloaded from SCIYO.COM

Dry friction on dampers is one of the main factors affecting ride comfort. For a vehicle traveling on a relatively smooth road at low speeds, the effect of road input cannot overcome dry friction force and, therefore, the suspensions are almost locked, which is known as Boulevard Jerk, and an uncomfortable vibration mode becomes effective due to reduced degrees of freedom (Silvester, 1966). Control of vibrations using non-linearity on active suspensions was achieved. (Alleyne et al., 1993) compared sliding mode controlled active suspensions with PID controlled active suspensions for a quarter car active suspension system. As the conclusion, the paper shows that sliding mode controller is better than PID one.
(Park & Kim, 2000) designed a decentralized variable structure controller for active suspension systems of vehicles. (Yokoyama et al., 2001) examined a new SMC for semi-active suspension systems with magneto-rheological (MR) dampers which have undesirable non-linear properties. (Yoshimura et al., 2001) showed the construction of an active suspension system for a quarter car model using the concept of sliding mode control. (Al-Holou et al., 2002) examined the development of a robust intelligent non-linear controller for active suspension systems based on a comprehensive and realistic non-linear model. (Guclu, 2004), (Guclu, 2005), (Guclu & Gulez, 2008) applied fuzzy logic controlled active suspensions on a non-linear four and eight degrees of freedom vehicle model without suspension-gap degeneration.
(Otten et al., 1997) applied for linear motors of a learning feed-forward controller.

2. Vehicle model

The non-linear full car model used in this study is shown in Figure 1. This full car model has eight degrees of freedom, namely vertical translations x_1, x_2, x_3, x_4, x_5, x_6 and angular rotations $x_7 = \theta$, $x_8 = \alpha$. These are the motion of the right front axle, the motion of the left front axle, the motion of the right rear axle, the motion of the left rear axle, the bounce motion of the passenger seat, the bounce motion of the vehicle body, the pitch motion of the vehicle body and the roll motion of the vehicle body, respectively. A passenger seat is included in the vehicle model to predict the response of the passenger due to a road disturbance. The common application in modeling the vehicle with a passenger seat is to add only one passenger seat preferably in the driver seat position though considering only one suspended seat implies that other seats are assumed to be fixed rigidly to the chassis (Baumal et al., 1998).
$f(Vr_i)$ is dry friction force. Namely, z_i (i = 1,…,4) in Figure 2 is road excitation and is given in Figure 7 in detail. y_i-x_i (i=1,…,5) represents relative displacements of the suspension systems and controllers. y_i is given in the Appendix. The equation of the linear motor is

$$R\,I + K_e(\dot{y}_i - \dot{x}_i) = v \qquad i = (1,\ldots,5) \tag{1}$$

where v and I are the control voltage and current of the armature coil, respectively. R and K_e are the resistance value and induced voltage constant of the armature coil. The current of the armature coil (I) and control force (u) has the following relation:

$$u = K_f\, I \tag{2}$$

K_f is the thrust constant. The inductance of the armature coil is neglected.
In general, the state-space form of a non-linear dynamic system can be written as follows:

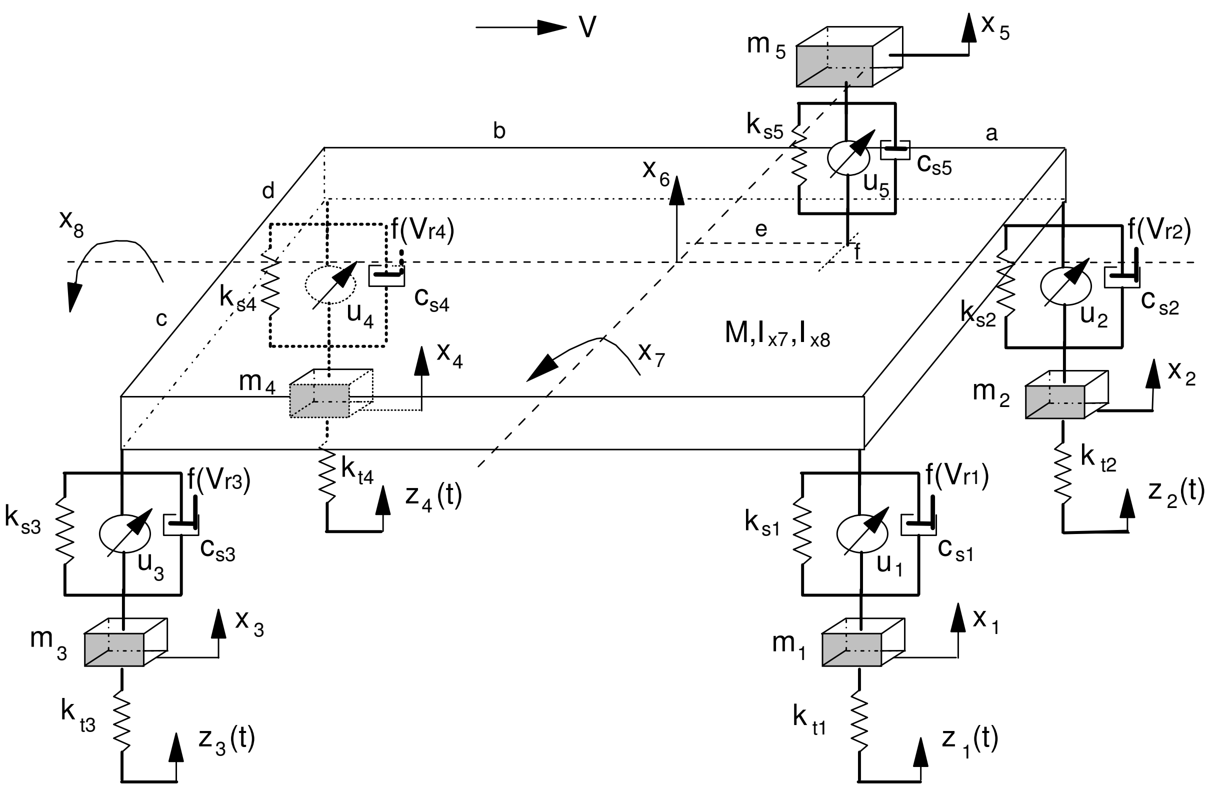

Fig. 1. The non-linear full car model with a passenger seat.

$$\underline{\dot{x}}=\underline{f}(\underline{x})+[B]\underline{u} \tag{3}$$

Here, for the eight degree-of-freedom system considered in this study, x = [x_1 x_2 x_3 .... x_{16}]^T where $x_9 = \dot{x}_1 = f_1(x)$, $x_{10} = \dot{x}_2 = f_2(x)$ and so on. $\underline{f}(\underline{x})$ is vector functions composed of first order differential equations that can be non-linear, [B] is the controller coefficient matrix and u = [u_1 u_2 u_3 u_4 u_5]^T is the control input vector written for the most general case in this study. $\underline{f}(\underline{x})$ and [B] are given in the Appendix along with the nomenclature of vehicle parameters. Mathematically, u_1, u_2, u_3 and u_4 do not have to exist together. In order to control vehicle body motions, three controller forces are sufficient since the body has three degrees of freedom in this study. These are bounce, pitch and roll motions. But, for practical reasons, four controllers parallel to the suspensions are introduced. The yaw motion is neglected. Finally, five controllers are used including the one under the passenger seat.

As mentioned before, the major non-linearity of the model comes from dry friction on the dampers. Geometric non-linearity has also been included. Dry friction on the dampers depends on the relative speed (V_r) between related damper ends. Experiments show that the dry friction model (Figure 2) has a viscous band character rather than being of a classical bang-bang type. The band ε is very small, and this prevents the complete locking of the suspension ends. For vehicle traveling with a low speed on a road with relatively low roughness generate dry friction force f(Vr) around ±R that practically locks the suspension generating a high equivalent viscous friction effect. Dry friction parameters are R=22 N and ε=0.0012 m/s.

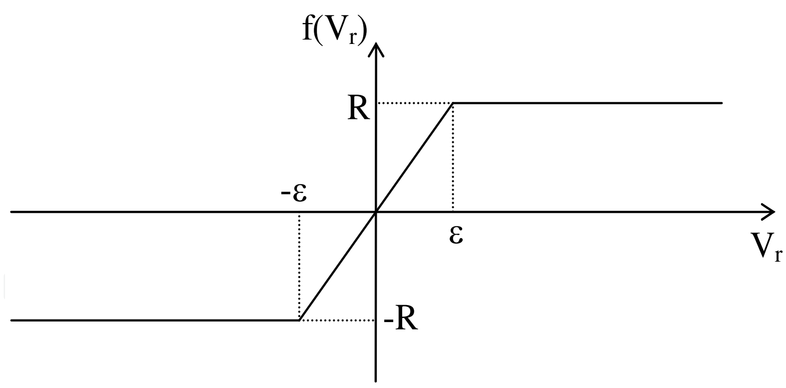

Fig. 2. Dry friction model

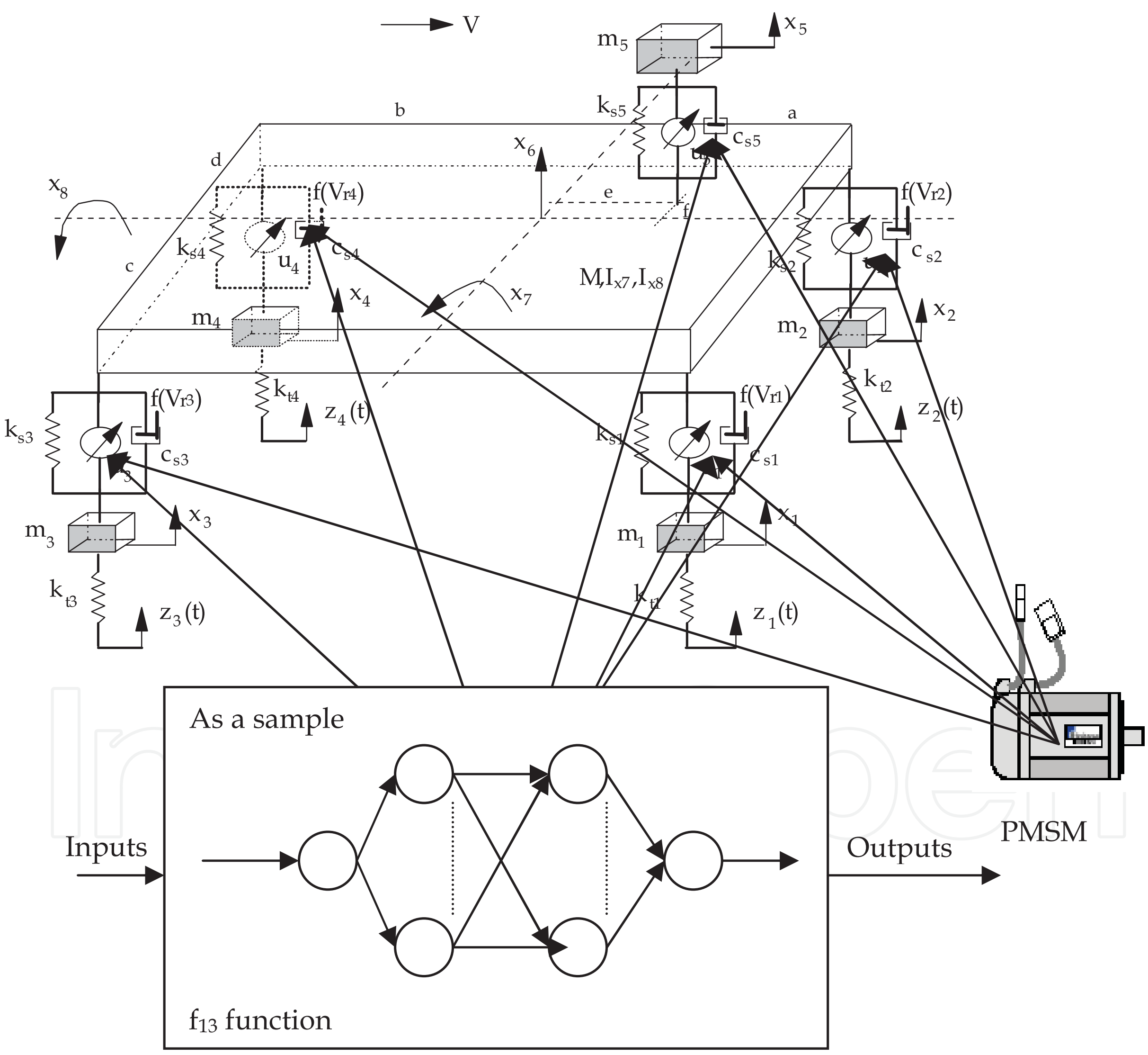

Fig. 3. The adaptation of NN controller closed form to the non-linear full vehicle model. Fast Back-propagation Algorithm (FBA) which is proposed by (Karayiannis & Venetsanopoulas, 1993) is used in the study.

3. Neural Network (NN) controller design

The Neural Network control is basically non-linear and adaptive in nature, giving robust performance under parameter variation and load disturbance effect. The main idea behind proposing a neural network controller on vehicles is its simplicity, satisfactory performance and the ability. Neural Networks are successfully used in variety applications areas such as control and early detection of machine faults. The feed-forward neural network is usually trained by a back-propagation training algorithm first proposed by (Rumelhart et al, 1986). This was the starting point of the effective usage of NNs after the 1980s. With the advantage of high speed computational technology, NNs are more realistic, easily updateable and implementable today. The distributed weights in the network contribute to the distributed intelligence or associative memory property of the network. The actual output pattern is compared with the desired output pattern and the weights are adjusted by the supervised back-propagation training algorithm until the pattern matching occurs, i.e., the pattern errors become acceptably small.

The impressive advantages of NNs are the capability of solving highly non-linear and complex problems and the efficiency of processing imprecise and noisy data.

Figure 3 shows the adaptation of the closed form of NN controller to the non-linear full car model with a passenger seat. The control forces are produced by PMSM.

4. Simulation part

In this study, the code of the tool written in C++ and Matlab with Simulink are used. The aim of the neural network control system for the vehicle system uses the functions from f_1 to f_{16} in the vehicle motions as the output variable while the variables of the other side of the equations of f_1-f_{16} in the Appendix are their inputs. Figure 4 shows the general operating block diagram of a NN algorithm.

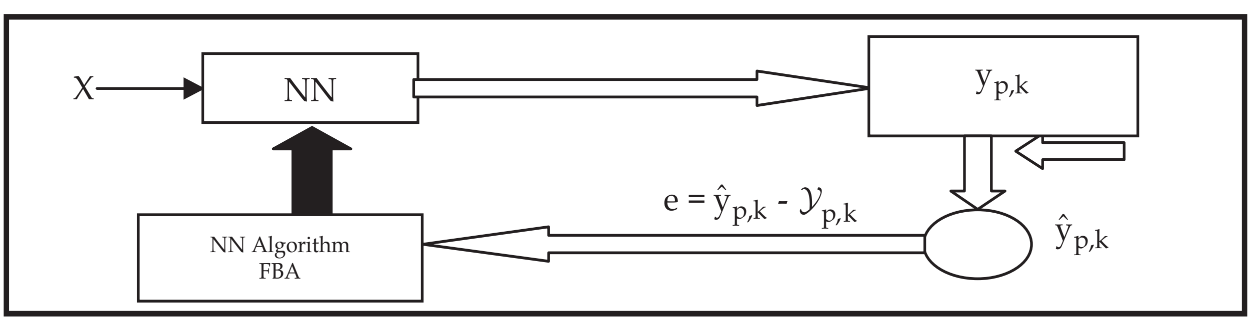

Fig. 4. Closed loop general block diagram of a neural network algorithm.

In this study, the FBA is used in the NN structure. The Neural Network input and output functions for the full vehicle system with passenger seat are given in Figure 5. The controllers have the following structures in Table 1.

In this study, NN controller is applied to a non-linear full vehicle model including Figure 5.

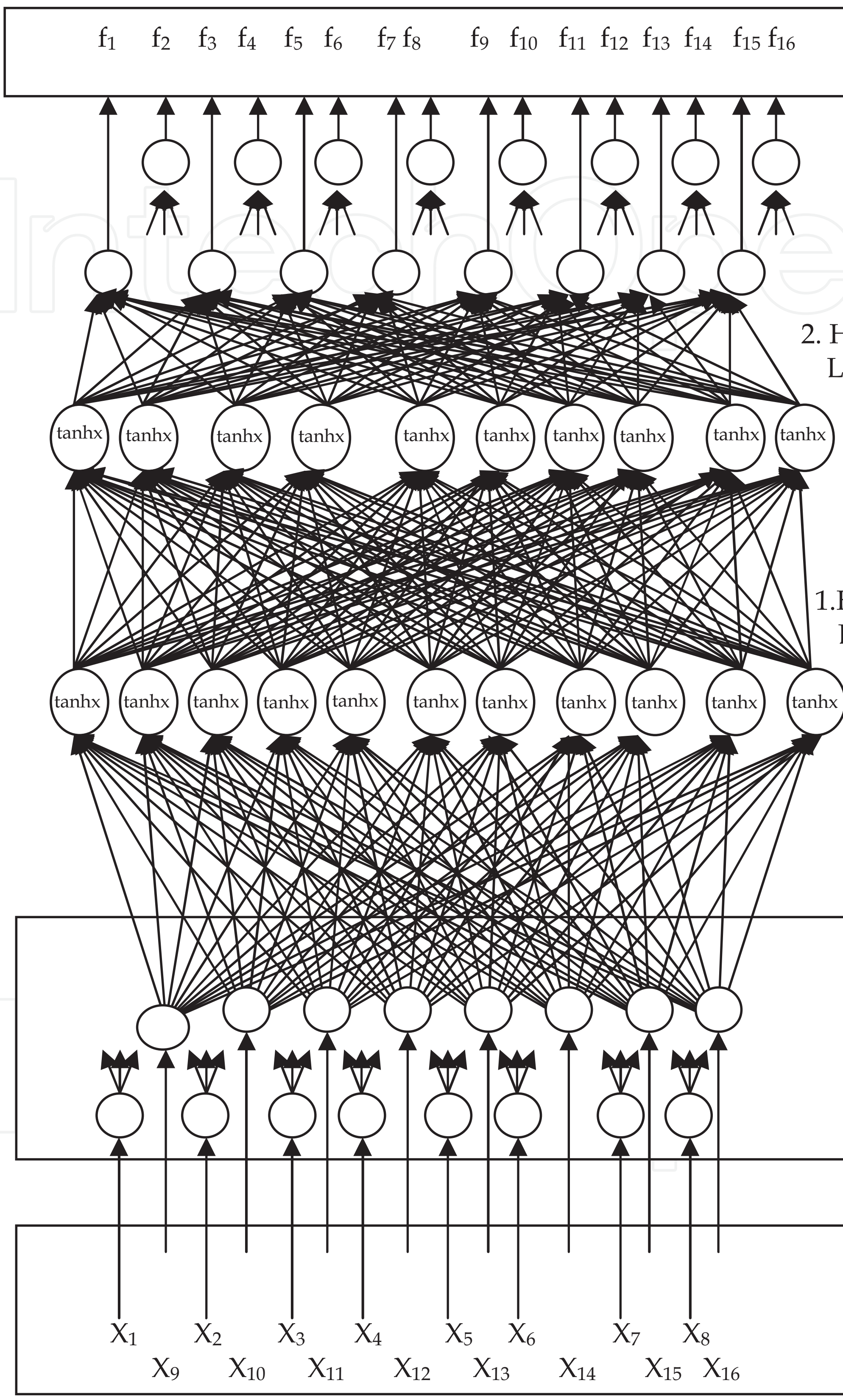

Fig. 5. Neural Network structure for the full vehicle control.

The Corresponding Variable	Number of Inputs	Number of Nodes in Hidden Layer-1	Number of Nodes in Hidden Layer-2	Number of Outputs	Generalized System Error (%)
f_1	1	4	3	1	0
f_2	1	4	3	1	0
f_3	1	4	3	1	0
f_4	1	4	3	1	0
f_5	1	4	3	1	0
f_6	1	4	3	1	0
f_7	1	4	3	1	0
f_8	1	4	3	1	0
f_9	7	10	9	1	0
f_{10}	7	10	9	1	0
f_{11}	8	11	10	1	0
f_{12}	8	11	10	1	0
f_{13}	6	9	8	1	0
f_{14}	15	18	17	1	0
f_{15}	15	18	17	1	0
f_{16}	15	18	17	1	0

Table 1. The structures of NN controllers for each function.

4.1 Time response of the non-linear vehicle model

In the simulation stage, first the non-linear model is used in order to obtain time responses. Second, for the frequency responses, the non-linear dry friction model is linearized using a describing function method. Accelerometers are used as sensors. These sensors are placed only to measure the states to be controlled. The data provided by these sensors are processed by micro-controllers having the NN algorithms designed. Here, the vehicle is assumed to travel over the bump road surface (Figure 6). The road bump parameters are h = 0.035 m and L = 0.025 m.

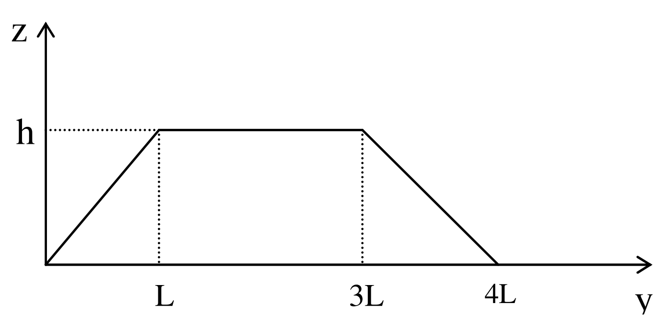

Fig. 6. Road disturbance.

There is a time delay between the front and rear wheel inputs. This time delay is as follows:

$$\delta(t) = (a + b)/V \tag{4}$$

where (a + b) is the distance between the front and rear axles and V is the velocity of the vehicle. Table 2 gives the NN test phase results for all functions, separately. Comparison diagrams of NN controller results and uncontrolled values are depicted in Figure 7. As to be seen from Table 2, all of the NN test phase results in Figure 7 are very good harmony with the uncontrolled ones. The momentum and learning rates are 0,7 and 0,9 respectively. The number of iteration for training phase is 3000000, and the number of hidden layer is 2. The

f_1 (x'_1)	f_1	f_2 (x'_2)	f_2	f_3 (x'_3)	f_3	f_4 (x'_4)	f_4
Uncont-rolled Values	NN Results	Uncont -rolled Values	NN Results	Uncont -rolled Values	NN Results	Uncont-rolled Values	NN Results
-0.2	-0.204308	-0.35	-0.3482	-0.0052	-0.004826	0.004	0.003139
0	0	-0.01	-0.010068	-0.0041	-0.003805	-0.0018	-0.001855
0	0	0	0	-0.0026	-0.002412	-0.0013	-0.001425
0	0	0	0	-0.0029	-0.002691	0.0018	0.001244
0	0	0	0	-0.0029	-0.002691	-0.0031	-0.002974
0	0	0	0	-0.0027	-0.002505	-0.002	-0.002027
0	0	0	0	0.001	0.00093	-0.0019	-0.001941

f_5 (x'_5)	f_5	f_6 (x'_6)	f_6	f_7 (θ')	f_7	f_8 (α')	f_8
Uncon-trolled Values	NN Results	Uncon-trolled Values	NN Results	Uncon-trolled Values	NN Results	Uncon-trolled Values	NN Results
0.017	0.016104	-0.028	-0.02744	0.1	0.098095	-0.006	-0.00573
0.007	0.006631	-0.001	-0.00098	-0.002	-0.001966	-0.004	-0.003822
0.012	0.011368	-0.001	-0.00098	-0.001	-0.000983	-0.001	-0.000959
-0.0025	-0.002371	0	0	0	0	0	-0.000004
0.0009	0.000851	0	0	0	0	0.001	0.00095
0	-0.000002	0	0	0	0	0	-0.000004
0	-0.000002	0	0	0	0	0	-0.000004

f_9 (x''_1)	f_9	f_{10} (x''_2)	f_{10}	f_{11} (x''_3)	f_{11}	f_{12} (x''_4)	f_{12}
Uncon-trolled Values	NN Results	Uncon-trolled Values	NN Results	Uncon-trolled Values	NN Results	Uncon-trolled Values	NN Results
-49.99911	-50	-15.01661	-15	-0.4	-0.399975	0.37	0.370004
-9.947977	-10	-7.896958	-8	-0.2	-0.199977	-0.3	-0.300001
-0.920222	0	-0.581933	0	0.63	0.688073	-0.56	-0.622842
-0.324225	0	-0.182448	0	-0.6	-0.613647	0.52	0.447904
-0.197652	0	-0.323465	0	-0.5	-0.541713	0.59	0.512811
-0.336008	0	-0.230341	0				

f_{13} (x''_5)	f_{13}	f_{14} (x''_6)	f_{14}	f_{15} (θ'')	f_{15}	f_{16} (α'')	f_{16}
Uncon-trolled Values	NN Results	Uncon-trolled Values	NN Results	Uncon-trolled Values	NN Results	Uncon-trolled Values	NN Results
0.13	0.13	-0.8	-0.8	-0.1	-0.099969	-0.25	-0.249997
-0.15	-0.15	-0.5	-0.499998	-0.05	-0.049979	0	0.000003
0.02	0.003019	0	-0.031477	0.1	0.081286	0.1	0.121414
0.01	0.00281	0	-0.000726	-0.001	-0.012811	0.02	0.02012
0	-0.01114	-0.001	0.000546	-0.0012	-0.002351	-0.001	0.001679
		-0.001	0.000443	-0.0012	0.000695	-0.0013	-0.005978
		-0.001	0.00035	-0.0012	-0.000332	-0.0013	0.001662

Table 2. The NN test phase results for all functions

number of hidden nodes in hidden layers are given in Table 1, respectively. The level of error shows that NN controller has a good approximation to control the system parameter and functions, since the generalized system error for all variables in Table 1 is % 0.

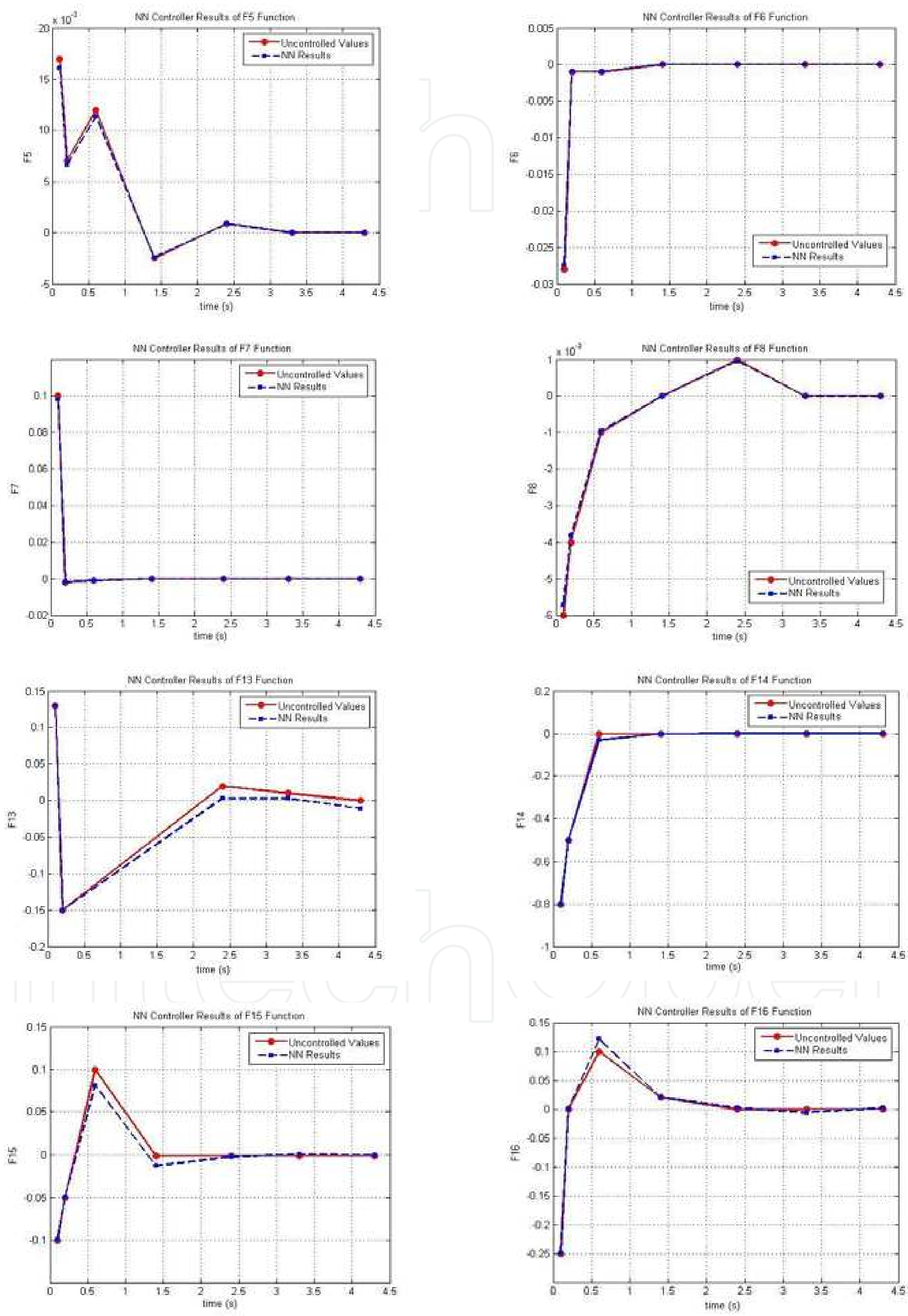

Fig. 7. Neural Network (NN) Controller results comparing with uncontrolled values.

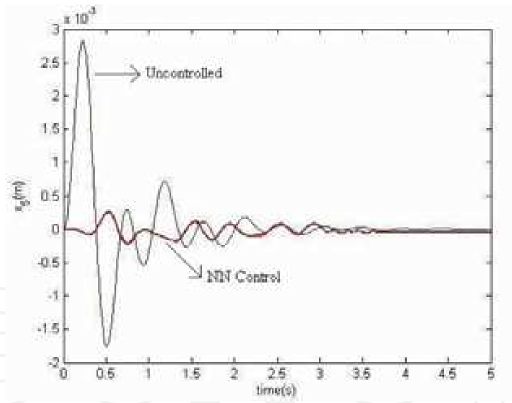

Fig. 8. Neural Network (NN) Controller results of passenger seat displacement for u_5=0.

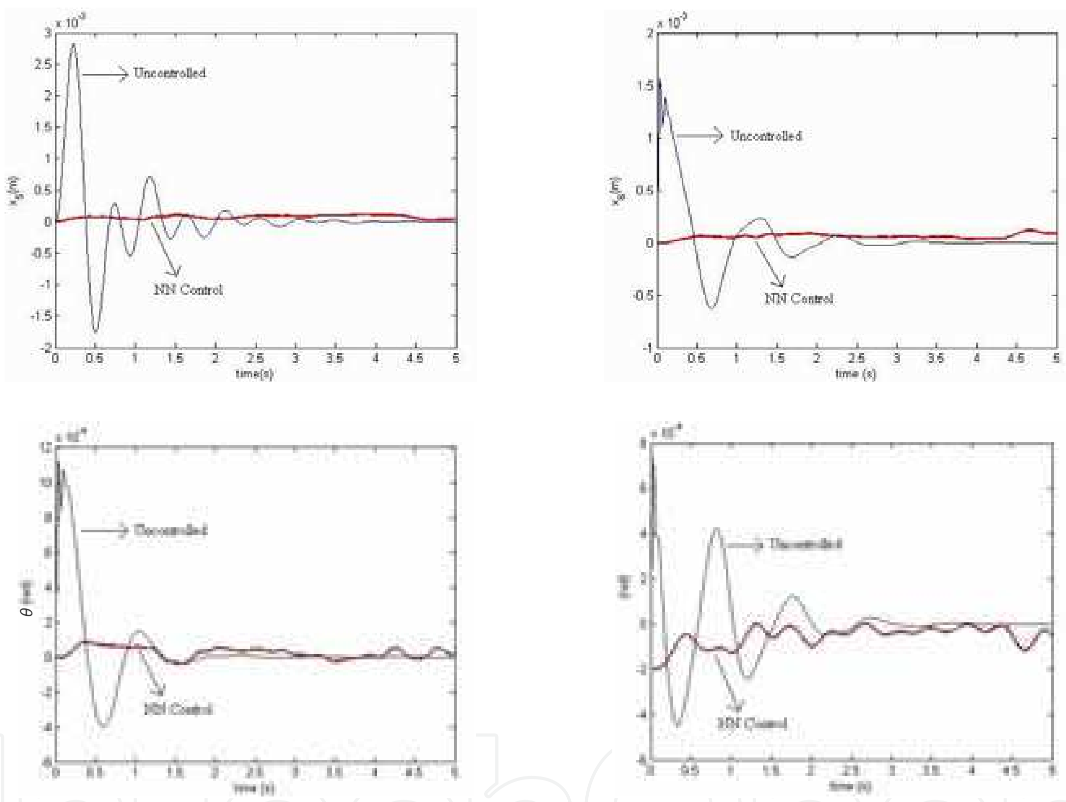

Fig. 9. Time responses of passenger seat and vehicle body displacements, pitch and roll angular displacements for controlled and uncontrolled cases.

"Figure 8 shows plot of x_5 without passenger seat controller (u_5=0). Since the other controllers are active, u_5 controller force of 9 N for the passenger seat is enough. If the seat controller is eliminated (u_5=0) and other controllers are kept, the results changes as in Figure 8." The time responses of passenger seat and vehicle body displacements, pitch and roll angular displacements for NN controlled and uncontrolled cases of the non-linear vehicle are shown in Figure 9. The maximum displacements of the active system are less than those of the passive system, and the active system returns to rest faster. All displacements are succesfully controlled by the proposed NN controller as well. The stick-slip effect of dry friction non-linearity having an offset in Figure 9 is observed for the uncontrolled case. This undesired effect is considerably overcome by NN controller as shown in the same figure.

"The passenger is almost isolated from the disturbance, since the all controllers are active. Here, maximum displacements of passenger seat for uncontrolled and NN controlled cases are $2,8.10^{-3}$ m and $0,2.10^{-3}$ m, respectively."

The vertical acceleration of the passenger is also an important criterion, which mainly affects ride comfort since the force generated by the inertia of the passenger creates disturbances. In other words, minimizing the vertical displacement may not mean an improvement in itself alone, as an improvement in the acceleration is also obtained. In Figure 10, the acceleration of the passenger in the non-linear vehicle model is shown. The NN controller decreases the amplitude of the acceleration when compared with the uncontrolled one.

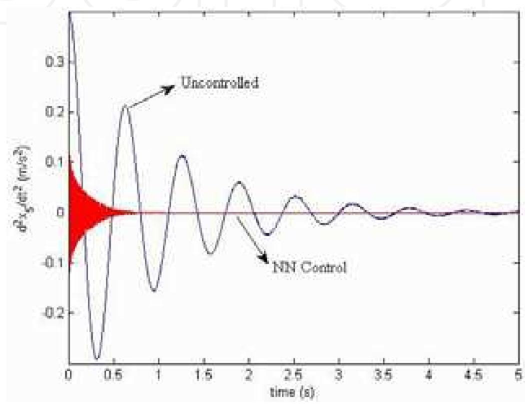

Fig. 10. Time responses of passenger seat vertical acceleration.

Another criterion is the control forces used since it is directly related with the cost of the controller. Figure 11 shows the controller force inputs. The front and rear suspensions apply a maximum force of about 4000 N. The amount of force applied to the passenger seat decreases since the body is controlled and the passenger seat is slightly isolated. A 9 N maximum force in addition to the other controller forces is sufficient to bring the passenger to the reference value of zero displacement.

4.2 Frequency response of the vehicle model

Frequency response analysis is the main tool in interpreting the dynamic behavior of vehicles. Since the frequency response plot of a non-linear system is dependent on input and is not unique, the dry friction model is linearized in frequency response analysis. Linearization without ignoring non-linearity is achieved by using the describing function method for dry friction on dampers and assuming that the vehicle body angular motions are small. In this technique, the effect of a non-linear dry friction model is replaced by a linear equivalent damping coefficient (C_e) obtained by the describing function method (Appendix). The frequency responses of the uncontrolled condition are compared with NN controller frequency response of the frame. In Figure 12, the frequency response plots of the passenger seat displacements and accelerations are considered. Two visual groups of displacement resonance frequencies in the uncontrolled case at approximately 2 and 15 Hz are observed in logarithmic plots. These frequencies belong to the vehicle system. In the NN controlled cases, the amplitudes of resonance frequencies of the vehicle system decrease. Actually, the vehicle model has eight resonance frequencies. The values of the related natural frequencies are obtained by solving the eigenvalue problem using Matlab. These values are 0.975, 1.183, 1.396, 2.202, 12.261, 12.264, 16.387 and 16.388 Hz. Since the natural frequencies are very close to each other, only two visual groups are seen in Figure 12. Using controllers under the vehicle body and passenger seat gives the maximum displacement and acceleration isolation for the passenger as shown in the figures.

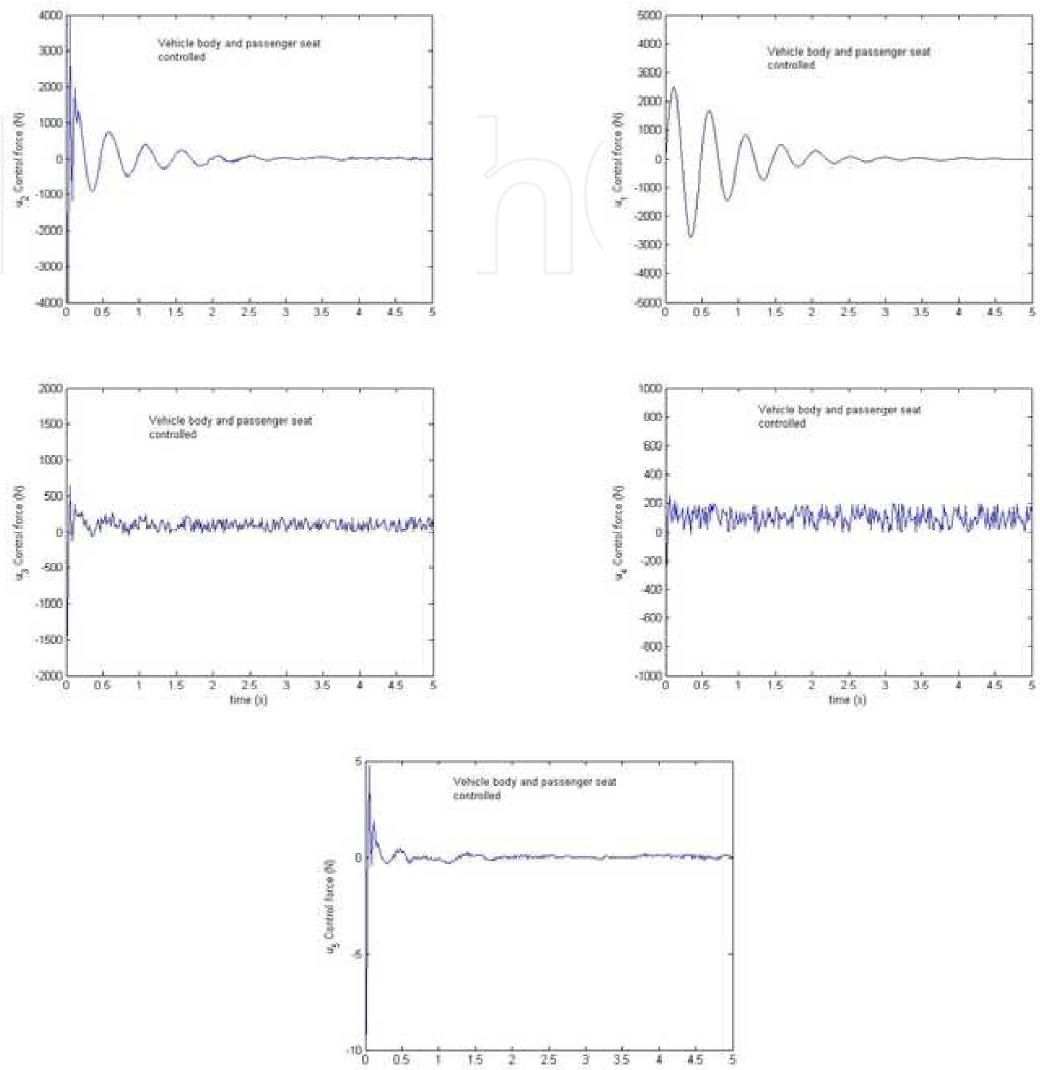

Fig. 11. NN Control force inputs.

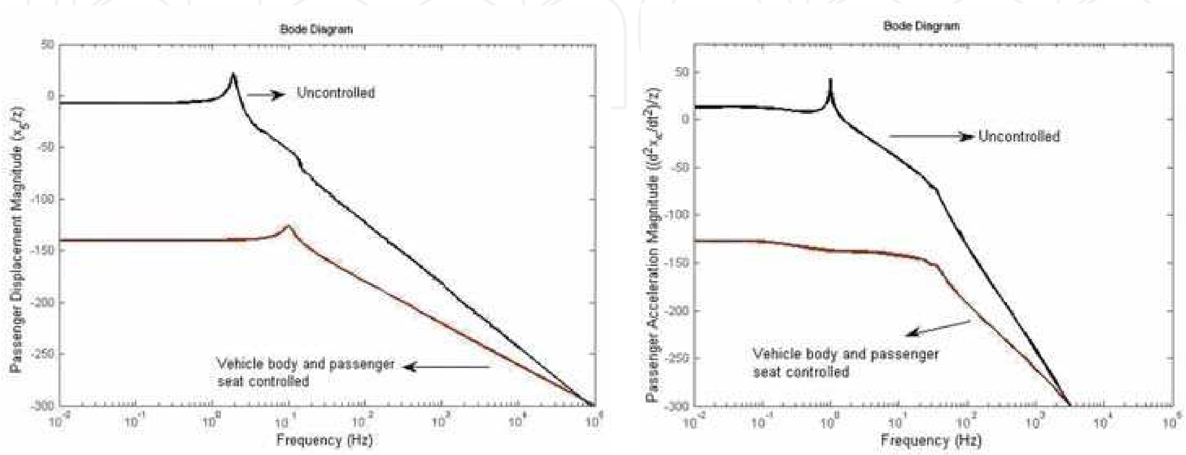

Fig. 12. Frequency response plots of passenger displacements and accelerations.

5. Conclusions

The aim of this study was the development of a Neural Network (NN) based controller for vibrations of a non-linear eight-degree-of-freedom vehicle model with active suspensions. This controller, which had a very good performance for the results both in time and frequency responses, has been applied to the vehicle. Only having controllers under the vehicle body without u_5 does not provide a good control over passenger comfort. The simulation results prove that, using controllers under the vehicle body and passenger seat provided excellent ride comfort. Therefore, this strategy should be taken into account by considering the control of the vehicle body and passenger seat together. Using this strategy, the bounce motion of the passenger reduces with an extra controller that applies very small force input, since the other controllers are active. If the passenger seat controller is eliminated and only other controllers are kept, the vibrations increase. A successful improvement has also been obtained in the isolation of the vertical acceleration of passengers. Frequency response plots of a passenger for this strategy support the results obtained. In conclusion, adding a controller under the passenger seat in addition to the other controllers improves ride comfort considerably. The decrease in vibration amplitudes and the excellent improvement in resonance values support this result.

6. Nomenclature

Vehicle variables

a , b	distances of axle to the center of gravity of the vehicle body (m)
c , d	distances of unsprung masses to the center of gravity of the axles (m)
e , f	distances of passenger seat to the center of gravity of the vehicle body (m)
c_{si}	ith damping coefficient of suspension (Ns/m)
c_{s5}	damping coefficient of passenger seat (Ns/m)
$f(V_{ri})$	ith dry friction force (N)
k_{si}	ith spring constant of suspension (N/m)
k_{s5}	spring constant of passenger seat (N/m)
k_{ti}	ith stiffness coefficient of tire (N/m)
m_i	ith mass of axle (kg)
m_5	mass of the passenger (kg)
x_i	ith state variable (m)
$z_i(t)$	ith road excitation (m)
I_{x7}	mass moment of inertia of the vehicle body for pitch motion (kgm2)
I_{x8}	mass moment of inertia of the vehicle body for roll motion (kgm2)
M	mass of the vehicle body (kg)

7. Appendix

The parameters of the vehicle:
$M = 1100$ kg
$I_{x7} = 1848$ kg.m^2
$I_{x8} = 550$ kg.m^2
$m_1 = m_2 = 25$ kg
$m_3 = m4 = 45$ kg
$m_5 = 90$ kg

$k_{s1} = k_{s2} = 15000$ N/m
$k_{s3} = k_{s4} = 17000$ N/m
$k_{s5} = 15000$ N/m
$c_{s1} = c_{s2} = c_{s3} = c_{s4} = 2500$ N.s/m
$c_{s5} = 150$ N.s/m
$k_{t1} = k_{t2} = k_{t3} = k_{t4} = 250000$ N/m
a = 1.2 m
b = 1.4 m
c = 0.5 m
d = 1.0 m
e = 0.3 m
f = 0.25 m
Dry friction force and linear equivalent damping coefficient:

$$f(Vr_i) = Ce_i(\dot{y}_i - \dot{x}_i) \qquad (i = 1...5)$$

$$Ce_i = \begin{cases} n & \text{if } \left|\dot{y}_i - \dot{x}_i\right| < \varepsilon \\ \dfrac{n}{\pi}(2\theta_i - \mathrm{Sin}2\theta_i) + \dfrac{4R}{\pi\left|\dot{y}_i - \dot{x}_i\right|}\mathrm{Cos}\theta_i & \text{else} \end{cases}$$

$$\theta_i = \mathrm{Sin}^{-1}\frac{\varepsilon}{\left|\dot{y}_i - \dot{x}_i\right|}$$

$$y_1 = x_6 + a\,\mathrm{Sin}\,x_7 - c\,\mathrm{Sin}\,x_8$$
$$y_2 = x_6 + a\,\mathrm{Sin}\,x_7 + d\,\mathrm{Sin}\,x_8$$
$$y_3 = x_6 - b\,\mathrm{Sin}\,x_7 - c\,\mathrm{Sin}\,x_8$$
$$y_4 = x_6 - b\,\mathrm{Sin}\,x_7 + d\,\mathrm{Sin}\,x_8$$
$$y_5 = x_6 + e\,\mathrm{Sin}\,x_7 + f\,\mathrm{Sin}\,x_8$$

State equations excluding control inputs:

$$f_1(x)=x_9 \quad , \quad f_2(x)=x_{10} \quad , \quad f_3(x)=x_{11} \quad , \quad f_4(x)=x_{12}$$
$$f_5(x)=x_{13} \quad , \quad f_6(x)=x_{14} \quad , \quad f_7(x)=x_{15} \quad , \quad f_8(x)=x_{16}$$

$$\begin{aligned} f_9(x)=1/m_1\,\{ &-(k_{s1}+k_{t1})x_1+k_{s1}x_6+a\,k_{s1}\,\mathrm{Sin}\,x_7-c\,k_{s1}\,\mathrm{Sin}\,x_8-c_{s1}x_9+c_{s1}x_{14} \\ &+a\,c_{s1}\mathrm{Cos}x_7\,x_{15}-c\,c_{s1}\,\mathrm{Cos}\,x_8\,x_{16}+k_{t1}z_1+f(V_{r1})-u_1 \} \end{aligned}$$

$$\begin{aligned} f_{10}(x)=1/m_2\,\{ &-(k_{s2}+k_{t2})x_2+k_{s2}x_6+a\,k_{s2}\,\mathrm{Sin}\,x_7+d\,k_{s2}\,\mathrm{Sin}\,x_8-c_{s2}x_{10}+c_{s2}x_{14} \\ &+a\,c_{s2}\mathrm{Cos}x_7\,x_{15}+d\,c_{s2}\,\mathrm{Cos}\,x_8\,x_{16}+k_{t2}z_2+f(V_{r2})-u_2 \} \end{aligned}$$

$$\begin{aligned} f_{11}(x)=1/m_3\,\{ &-(k_{s3}+k_{t3})x_3+k_{s3}x_6-b\,k_{s3}\,\mathrm{Sin}\,x_7-c\,k_{s3}\,\mathrm{Sin}\,x_8-c_{s3}x_{11}+c_{s3}x_{14} \\ &-b\,c_{s3}\mathrm{Cos}x_7\,x_{15}-c\,c_{s3}\,\mathrm{Cos}\,x_8\,x_{16}+k_{t3}z_3+f(V_{r3})-u_3 \} \end{aligned}$$

$$\begin{aligned} f_{12}(x)=1/m_4\,\{ &-(k_{s4}+k_{t4})x_4+k_{s4}x_6-b\,k_{s4}\,\mathrm{Sin}\,x_7+d\,k_{s4}\,\mathrm{Sin}\,x_8-c_{s4}x_{12}+c_{s4}x_{14} \\ &-b\,c_{s4}\mathrm{Cos}x_7\,x_{15}+d\,c_{s4}\,\mathrm{Cos}\,x_8\,x_{16}+k_{t4}z_4+f(V_{r4})-u_4 \} \end{aligned}$$

$$\begin{aligned} f_{13}(x)=1/m_5\,\{ &-k_{s5}x_5+k_{s5}x_6+e\,k_{s5}\,\mathrm{Sin}\,x_7+f\,k_{s5}\,\mathrm{Sin}\,x_8-c_{s5}x_{14}+c_{s5}x_{14} \\ &+e\,c_{s5}\mathrm{Cos}x_7\,x_{15}+f\,c_{s5}\,\mathrm{Cos}\,x_8\,x_{16}+u_5 \} \end{aligned}$$

$$\begin{aligned}
f_{14}(x)=1/M\,\{ & k_{s1}x_1+k_{s2}x_2+k_{s3}x_3+k_{s4}x_4+k_{s5}x_5-\left(k_{s1}+k_{s2}+k_{s3}+k_{s4}+k_{s5}\right)x_6 \\
& -\left(a\left(k_{s1}+k_{s2}\right)-b\left(k_{s3}+k_{s4}\right)+ek_{s5}\right)\mathrm{Sin}\,x_7-(d(k_{s2}+k_{s4})-c(k_{s1}+k_{s3})+fk_{s5})\mathrm{Sin}\,x_8 \\
& +c_{s1}x_9+c_{s2}x_{10}+c_{s3}x_{11}+c_{s4}x_{12}+c_{s5}x_{13}-(c_{s1}+c_{s2}+c_{s3}+c_{s4}+c_{s5})x_{14} \\
& -\left(a\left(c_{s1}+c_{s2}\right)-b\left(c_{s3}+c_{s4}\right)+ec_{s5}\right)\mathrm{Cos}\,x_7x_{15}-(d(c_{s2}+c_{s4})-c(c_{s1}+c_{s3})+fc_{s5})\mathrm{Cos}\,x_8x_{16} \\
& -f\left(V_{r1}\right)-f\left(V_{r2}\right)-f\left(V_{r3}\right)-f\left(V_{r4}\right)+u_1+u_2+u_3+u_4-u_5\,\}
\end{aligned}$$

$$\begin{aligned}
f_{15}(x)=1/I_{x7}\{ & ak_{s1}x_1+ak_{s2}x_2-bk_{s3}x_3-bk_{s4}x_4+ek_{s5}x_5-\left(a\left(k_{s1}+k_{s2}\right)-b\left(k_{s3}+k_{s4}\right)+ek_{s5}\right)x_6 \\
& -\left(a^2\left(k_{s1}+k_{s2}\right)+b^2\left(k_{s3}+k_{s4}\right)+e^2k_{s5}\right)\mathrm{Sin}x_7-(d(ak_{s2}-bk_{s4})-c(ak_{s1}-bk_{s3})+efk_{s5})\mathrm{Sin}x_8 \\
& +ac_{s1}x_9+ac_{s2}x_{10}-bc_{s3}x_{11}-bc_{s4}x_{12}+ec_{s5}x_{13}-\left(a\left(c_{s1}+c_{s2}\right)-b\left(c_{s3}+c_{s4}\right)+ec_{s5}\right)x_{14} \\
& -\left(a^2\left(c_{s1}+c_{s2}\right)+b^2\left(c_{s3}+c_{s4}\right)+e^2c_{s5}\right)\mathrm{Cos}x_7x_{15}-(d(ac_{s2}-bc_{s4})-c(ac_{s1}-bc_{s3})+efc_{s5})\mathrm{Cos}x_8x_{16} \\
& -af\left(V_{r1}\right)-af\left(V_{r2}\right)+bf\left(V_{r3}\right)+bf\left(V_{r4}\right)+a(u_1+u_2)-b(u_3+u_4)-eu_5\,\}\,\mathrm{Cos}\,x_7
\end{aligned}$$

$$\begin{aligned}
f_{16}(x)=1/I_{x8}\{ & -ck_{s1}x_1+dk_{s2}x_2-ck_{s3}x_3+dk_{s4}x_4+fk_{s5}x_5-\left(d\left(k_{s2}+k_{s4}\right)-c\left(k_{s1}+k_{s3}\right)+fk_{s5}\right)x_6 \\
& -\left(d\left(ak_{s2}-bk_{s4}\right)-c\left(ak_{s1}-bk_{s3}\right)+efk_{s5}\right)\mathrm{Sin}x_7-(d^2(k_{s2}+k_{s4})+c^2(k_{s1}+k_{s3})+f^2k_{s5})\mathrm{Sin}x_8 \\
& -cc_{s1}x_9+dc_{s2}x_{10}-cc_{s3}x_{11}+dc_{s4}x_{12}+fc_{s5}x_{13}-\left(d\left(c_{s2}+c_{s4}\right)-c\left(c_{s1}+c_{s3}\right)+fc_{s5}\right)x_{14} \\
& -\left(d\left(ac_{s2}-bc_{s4}\right)-c\left(ac_{s1}-bc_{s3}\right)+efc_{s5}\right)\mathrm{Cos}\,x_7x_{15}-(d^2(c_{s2}+c_{s4})+c^2(c_{s1}+c_{s3})+f^2c_{s5})\mathrm{Cos}\,x_8x_{16} \\
& -c\,f\left(V_{r1}\right)+df\left(V_{r2}\right)-cf\left(V_{r3}\right)+df\left(V_{r4}\right)-c(u_1+u_3)+d(u_2+u_4)-fu_5\,\}\,\mathrm{Cos}\,x_8
\end{aligned}$$

The controller force matrix:

$$[B]=\begin{bmatrix}
0 & 0 & 0 & 0 \\
0 & 0 & 0 & 0 \\
0 & 0 & 0 & 0 \\
0 & 0 & 0 & 0 \\
0 & 0 & 0 & 0 \\
0 & 0 & 0 & 0 \\
0 & 0 & 0 & 0 \\
0 & 0 & 0 & 0 \\
-\dfrac{bd}{(a+b)(c+d)m_1} & -\dfrac{d}{(a+b)(c+d)m_1} & \dfrac{1}{(c+d)m_1} & \dfrac{-d(b+e)+f(a+b)}{(a+b)(c+d)m_1} \\
-\dfrac{bc}{(a+b)(c+d)m_2} & -\dfrac{c}{(a+b)(c+d)m_2} & -\dfrac{1}{(c+d)m_2} & \dfrac{-c(b+e)-f(a+b)}{(a+b)(c+d)m_2} \\
-\dfrac{ad}{(a+b)(c+d)m_3} & \dfrac{d}{(a+b)(c+d)m_3} & 0 & -\dfrac{d(a-e)}{(a+b)(c+d)m_3} \\
-\dfrac{ac}{(a+b)(c+d)m_4} & \dfrac{c}{(a+b)(c+d)m_4} & 0 & -\dfrac{c(a-e)}{(a+b)(c+d)m_4} \\
0 & 0 & 0 & \dfrac{1}{m_5} \\
\dfrac{1}{M} & 0 & 0 & 0 \\
0 & \dfrac{1}{I_{x7}} & 0 & 0 \\
0 & 0 & \dfrac{1}{I_{x8}} & 0
\end{bmatrix}$$

8. References

Redfield, R.C. & Karnopp, D.C. (1988). Optimal performance of variable component suspensions, *Vehicle System Dynamics* 17, pp 231-253.

Yue, C.; Butsuen, T. & Hedrick, J.K. (1989). Alternative control laws for automotive active suspensions, *Journal of Dynamic Systems, Measurement and Control* 111, pp. 286-291

Stein, G.J. & Ballo, I. (1991). Active vibration control system for the driver's seat for off-road vehicles, *Vehicle System Dynamics* 20, pp. 57-78.

Hac, A. (1992). Optimal linear preview control of active vehicle suspension, *Vehicle System Dynamics* 21, pp. 167-195.

Rakheja, S., Afework, Y. & Sankar, S. (1994). An analytical and experimental investigation of the driver-seat-suspension system, *Vehicle System Dynamics* 23, pp. 501-524.

Crolla, D.A. & Abdel Hady, M.B.A.,(1991). Active suspension control; Performance comparisons using control laws applied to a full car model, *Vehicle System Dynamics* 20, pp. 107-120.

Hrovat, D. (1993). Applications of optimal control to advanced automotive suspension design, *Journal of Dynamic Systems, Measurement, and Control* 115, 328-342.

Silvester, B.C. (1966). Vibration reduction in motor cars, *Soc. Environmental Engineers* 4.

Alleyne, A.; Neuhaus, P.D. & Hedrick, J.K. (1993). Application of non-linear control theory to electronically controlled suspensions, *Vehicle System Dynamics* 22, pp. 309-320.

Park, J.H. & Kim, Y.S. (2000). Decentralized variable structure control of vehicle active suspensions, *JSME Mech. Systems, Machine Elements, Manufacturing* 43(1), pp. 73-79.

Yokoyama, M.; Hedrick, J.K. & Toyama, S.(2001). A model following sliding mode controller for semi-active suspension systems with MR dampers, in *Proceedings of the American Control Conference*, pp. 2652-2657, Arlington, VA, 4, June 25-27.

Yoshimura, T.; Kume, A.; Kurimoto, M. & Hino, J. (2001). Construction of an active suspension system of a quarter car model using the concept of sliding mode control, *Journal of Sound and Vibration* 239(2), pp. 187-199.

Al-Holou, N.; Lahdhiri, T.; Joo, D.S.; Weaver, J. & Al-Abbas, F. (2002). Sliding mode neural network inference fuzzy logic control for active suspension systems, *IEEE Transactions on Fuzzy Systems* 10(2), pp. 234-246.

Guclu, R. (2004). The Fuzzy Logic control of active suspensions without suspension-gap degeneration, *Strojniski Vestnik*, 50, pp. 462-468.

Guclu, R. (2005) Fuzzy Logic control of seat vibrations of a non-linear full vehicle model, *Nonlinear Dynamics,* 40, pp. 21-34.

Guclu, R., Gulez K. (2008). Neural Network Control of Seat Vibrations of a Non-linear Full Vehicle Model using PMSM, *Mathematical and Computer Modelling*, 47(11-12), pp.1356-1371.

Otten, G.; de Vries, T.J.A.; Rankers, A.M. & Gaal, E.W. (1997). Linear motor motion control using a learning feedforward controller, *IEEE Transactions on Mechatronics*, 2(3).

Baumal, A.E.; McPhee, J.J. & Calamai, P.H. (1998). Application of genetic algorithms to the design optimization of an active vehicle suspension system, *Computer Methods in Applied Mechanics and Engineering* 163, pp. 87-94.

Rumelhart, D. E.; Hinton , G. E & Williams, R. J. (1986). Learning representations by back-propagation errors, *Nature* 323, pp. 533-536.

Karayiannis, N.B. & Venetsanopoulas A.N. (1993). In: *Artificial Neural Networks- Learning Algorithms, Performance Evaluation and Applications,* Kluwer Academic Publishers.

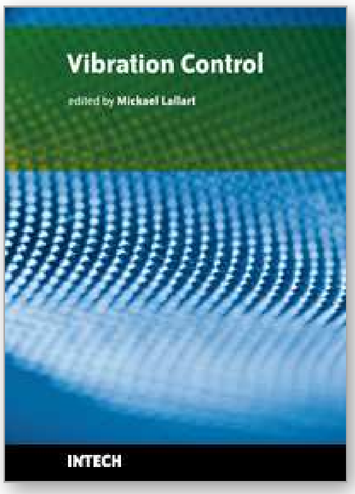

Vibration Control
Edited by MickaÃƒÂ«l Lallart

ISBN 978-953-307-117-6
Hard cover, 380 pages
Publisher Sciyo
Published online 18, August, 2010
Published in print edition August, 2010

Vibrations are a part of our environment and daily life. Many of them are useful and are needed for many purposes, one of the best example being the hearing system. Nevertheless, vibrations are often undesirable and have to be suppressed or reduced, as they may be harmful to structures by generating damages or compromise the comfort of users through noise generation of mechanical wave transmission to the body. the purpose of this book is to present basic and advanced methods for efficiently controlling the vibrations and limiting their effects. Open-access publishing is an extraordinary opportunity for a wide dissemination of high quality research. This book is not an exception to this, and I am proud to introduce the works performed by experts from all over the world.

InTech Europe
University Campus STeP Ri
Slavka Krautzeka 83/A
51000 Rijeka, Croatia
Phone: +385 (51) 770 447
Fax: +385 (51) 686 166
www.intechopen.com

InTech China
Unit 405, Office Block, Hotel Equatorial Shanghai
No.65, Yan An Road (West), Shanghai, 200040, China
中国上海市延安西路65号上海国际贵都大饭店办公楼405单元
Phone: +86-21-62489820
Fax: +86-21-62489821